Compression after impact fatigue delamination propagation control using discrete interleaved crack arrest films

M. Yasaee, C. Killock, J. Hartley, I.P. Bond

Advanced Composites Centre for Innovation and Science (ACCIS), University of Bristol, Queen's Building, University Walk, Bristol, BS8 1TR, UK

Keywords

Abstract

A novel delamination damage control and management concept is demonstrated showing how, through selective placement of discrete thermoplastic film interleaves, it is possible to manipulate the formation of impact damage and control its subsequent propagation during compressive fatigue cyclic loading.

This process has been shown to significantly improve the fatigue life of the composite panels tested by an average of 13 times. It is proposed that this method of controlling delamination damage growth may lead to lower weight damage tolerant composite designs resulting in more cost effective composite structures.

1. Introduction

The excellent specific properties of fibre reinforced polymer (FRP) composites make them an ideal material for use in lightweight structures. However, their potential for more widespread use is constrained by several shortcomings, including their lack of ductility and poor out of plane performance. A typical FRP structure comprises of stacked layers, with the fibres arranged within the plane of these layers. The lack of any through thickness reinforcement leads to relatively easy formation of delamination damage, which severely degrades the global performance of the material. Even minor impact damage can result in reductions of up to 35% in residual strength [1]. For this reason, laminated composite structures that have sustained delamination damage are deemed as failed components and are either repaired or replaced. This has led to constrained composite designs that try to mitigate the delamination failure mode, which typically leads to conservative design allowables or excessively heavy components.

If delamination damage could be contained or 'compartmentalised' and its propagation effectively managed, considerable weight and cost savings could be attained and more innovative FRP designs may be realised. Studies exist in the literature aimed at resisting delamination growth by improving the toughness of the parent resin, through thickness reinforcements in the form of pinning [2,3], stitching and tufting [4] and interleaving tough constituents [5,6]. Each technique offers various advantages, however, there still exist deficiencies in all these approaches. Through thickness reinforcement significantly improves delamination resistance, however, manufacturing and material costs, as well as their propensity to generate defects which result in severe reduction of in-plane properties, has led to its limited use [7]. Interleaving tough constituents is an effective process of increasing

delamination resistance; however, liberal use of these materials may result in lower global stiffness, strength and adverse effects on the global fibre volume fraction of the composite. Therefore, additional plies must be introduced to counter such reductions, which in turn results in increased mass [8].

For this reason, a proposal to use interleaving materials but in a discrete form will still offer localised resistance to delamination growth [5,6] yet maintain the global properties of the composite. Yasaee et al. [9] showed that by selectively implementing these discrete films in a laminated composite panel, it is not only possible to suppress delamination damage but also to control and promote delamination in various forms. This bio-inspired process termed 'compartmentalisation' was shown to effectively increase the compressive strength of an impact damaged composite laminate.

In this study, the same technique is implemented to highlight the potential concept of delamination damage management to significantly improve composite performance even in the presence of delamination damage growth under cyclic loading.

2. Concept

An illustration of the delamination propagation control concept is shown in Figure 1. In this scenario, discrete interleaved crack arresting films arranged in a grid pattern have been embedded within a laminated composite panel. When subjected to a low velocity impact, the damage that is formed is contained within a predetermined region. Subsequent prolonged exposure to compression fatigue cycles will result in growth of this damage. However, this growth is resisted in all directions (presence of interleaves) with the exception of propagation to the left of the panel (no interleave). This can be beneficial since damage propagation can be directed away from high stress regions or in this case towards a region where a multifunctional vascular

network capable of self-healing has been incorporated. Once this damage interacts with these vascular networks, it will then be possible to autonomously infuse a healing agent into the damaged area to achieve some form of mechanical property recovery. In this study, feasibility of the concept for controlling delamination propagation under cyclic loading is investigated by effectively steering crack growth in a composite panel, Figure 1, in a pre-determined direction.

3. Materials

A 16-ply composite laminate of pre-impregnated E-glass/913 epoxy (Hexcel, UK) was selected and cured according to manufacturer's recommendations. The laminate stacking sequence of $[(45)_2, (90)_2, (-45)_2, (0)_2]_S$ was selected to make a 2.33mm±0.05 thick quasi-isotropic panel. The 0° plies are orientated to be coincident with the compression loading described later. A double ply configuration was chosen to reduce the number of potential inter-ply delamination locations hence simplifying the design and manufacturing process.

Two configurations were designed for the panels with the crack redirection features as shown in Figure 2. The embedded interleaved strips were made from thermoplastic copolymer Poly (Ethylene-co-MethAcrylic Acid) or EMAA. Initially acquired in pellet form from Sigma-Aldrich, they were then formed into films of approximately 100μm±25. These films were cut into 2.5mm strips and positioned between selected plies as shown in Figure 2, according to the interleaved stacking sequence shown in

Table 1.

The *straight* configuration is designed such that the strips suppress any damage formation to the right of the impact point and only allow damage growth during fatigue towards the left side of the panel. The *grid* configuration was designed so as to constrain damage within a specified region or 'compartment' and only allow damage propagation during fatigue towards the left side of the panel within the bounds of the interleaved region.

4. Methods

An Instron Dynatup 9250HV drop weight tower was used to generate the low velocity impact event according to the guidelines set out in ASTM-D7136 [10]. Each specimen was clamped into the impact support fixture which contained a 75mm by 125mm window cut out. Each specimen was orientated such that the 0° fibre direction was parallel to the 75mm length of the window and was impacted with a 20mm diameter hemispherical striker tip to generate 15J of energy upon contact. Eight replicates of each configuration were tested.

Each specimen was assessed using optical microscopy and non-destructive evaluation (NDE) ultrasonic C-scan testing (USL SAM 350 fitted with a NDT UPR receiver and a Panametrics V311 10 MHz/0.500 transducer). Each damaged specimen was then cut into panel sizes of 89mm by 55mm with the impact point directly at the centre of the panel. They were then placed into an anti-buckling support fixture similar to that detailed in ASTM-D7137 [11] but modified to accommodate smaller panels, as outlined by Prichard and Hogg [1].

Three replicates of each configuration were subject to a static compressive load under displacement control at a rate of 0.4mm/min until failure occurred. This test was necessary to determine the residual compressive strength of the baseline double ply configuration, following 15J impact.

The remaining five specimens were then subject to 5 Hz compression-compression cyclic loading (R=11) at approximately 81% residual compressive strength until failure.

5. Results

5.1. Low velocity impact damage area

The resulting 15J impact damage area for the *control*, *straight* and *grid* configurations are presented in Figure 3, Figure 4 and Figure 5 respectively. The control panel clearly exhibits the typical post-impact staircase delamination pattern commonly observed in multidirectional laminates [12]. Only four interfaces were found to have delaminated with the largest occurring towards the back face.

The *straight* configuration clearly shows arrest of delaminations to the right of the impact point. The *grid* configuration exhibits compartmentalised delaminations above, below and to the right of the impact location. The average plan-form impact damage area for the *control*, *straight* and *grid* configurations were 409(±9)mm^2, 358(±14)mm^2 and 294(±12)mm^2 respectively.

5.2. Static compression

The average compression after impact (CAI) strength and damage footprint area of the three configurations subjected to 15J impact are presented in Figure 6. The compression strength of an undamaged panel was not measured since it has been

shown that a pristine panel will typically result in failure at or near the loading grips [1]. The control panel exhibited an average strength of 213MPa with average damage footprint area of 409mm^2. The *straight* and the *grid* configuration both exhibited reduced impact damage area of up to 13% and 26%, respectively. However, the CAI strength does not appear to reflect this improvement as both exhibit strengths of 223MPa and 214MPa within the scatter of the control samples.

This uncharacteristic response has been observed previously in impact scenarios where plates with dissimilar damage sizes have exhibited similar CAI strengths [9]. The reason for this behaviour is due to the delamination interface location and the influence this has on the buckling behaviour of the composite [13]. For an unmodified laminate the impact delamination pattern is well understood, thereby CAI strength can be reasonably predicted [14]. However, when the delamination pattern is manipulated, the varying delamination location and non-monotonic impact damage areas cannot be used to accurately predict the resulting CAI strength of the material.

5.3.Fatigue compression

Fatigue CAI tests were performed on the remaining samples using the same test fixture. Sinusoidal compressive to compressive (C-C) cyclic loading was applied to the specimens between 2kN to 22kN (fatigue ratio R=11) at a frequency of 5Hz. These load levels correspond to approximately 81% of the post-impact residual compression strength of the unmodified control configuration panel. Figure 7 highlights the behaviour of the impact induced damage growth of the *control* panel when subjected to the C-C cyclic loading. Delamination began propagating in the 90°/45° interface nearest the back face. At approximately 42,000 cycles, the delamination reaches the anti-buckling guide boundaries. At this point, the

delamination began to grow towards the centre. After the separate delaminations began to connect through the middle of the panel (~59,000 cycles), new delaminations were initiated at interfaces near to the mid-plane, eventually leading to buckling failure (69,000 cycles). Similar response was seen across the four samples tested, giving average cycles to failure of approximately 54,000 cycles.

The *straight* configuration response to fatigue cycle is shown in Figure 8. The delamination growth occurred on the 90°/45° interface nearer to the back face, similar to the *control* panel. However, the *straight* interleaved strip clearly prevented any damage growth to the right hand side of the panel. The delamination took ~156,000 cycles to reach the anti-buckling guide boundaries, followed by delamination growth towards the centre. By 183,000 cycles, new delaminations began propagating at interfaces near the mid-plane which led to a sudden loss of stiffness in the mid-section resulting in failure. All straight configuration samples showed similar response giving average cycles to failure of 150,000.

The *grid* configuration response to fatigue loading is shown in Figure 9. For large number of cycles, the delamination remained intact with little or no growth. In the sample shown after approximately 1,000,000 cycles, delamination slowly began to grow towards the top until arrested at the horizontal interleaved strips, which then promoted growth in the lateral direction until failure. All *grid* configuration samples showed similar response giving average lifetime to failure of 730,000 cycles.

It is interesting to observe that the initial delamination propagation of the *control* and *straight* sample occurred on interface 6 (

Table 1) and that this growth is seen to be less influential on global stiffness response than the delamination growth in the interfaces closer to the mid-plane. In all three configurations, once delamination began to grow at the interfaces near the mid-plane, global failure was reached a few thousand cycles later.

A summary of the C-C fatigue results are provided in Table 2. A plot of stiffness degradation against fatigue cycles is presented in Figure 10. All curves show large reduction in stiffness during the initial 20,000 cycles. This may be the result of stabilisation of the samples in the fixture grips. Following this initial stabilisation, the *control* samples showed a large almost constant rate of reduction in stiffness until complete failure. The *straight* configuration exhibited a more gradual loss of stiffness after initial stabilisation until failure. These stiffness losses can be attributed to the growth of the damage on the back face. Since the *straight* configuration only showed delamination growth in one direction, the loss in stiffness was less critical than in the *control* samples.

The *grid* configuration did not exhibit any delamination growth for prolonged periods. This is reflected in a very small reduction in stiffness. The delamination that eventually did propagate on the mid-ply interfaces triggered accelerated failure.

6. Discussion

A concept for compartmentalising and controlling the direction of damage propagation has been shown. The embedded thermoplastic films arranged in a simple *straight* configuration were able to constrain delamination propagation within the panel and promote growth in a desired direction. In a more complex *grid* like configuration, the damage was effectively compartmentalised and no evidence of damage growth outside the grid constraint was observed following extensive fatigue

loading. More significantly, the fatigue life was significantly enhanced relative to an unmodified *control* panel, given that the static CAI strength of the three configurations was very similar.

To achieve the same fatigue life improvements, without modifications, would require heavier laminate designs. This clearly highlights the potential benefits of managing damage compared to the current conservative 'no growth' approach.

The tests carried out in this study were performed on a specimen of relatively limited dimensions. In all cases, damage growth was observed to eventually interact with the boundaries of the support fixture, thereby altering the damage propagation mechanisms. This may have been a contributing factor in the subsequent failure of the panels, and may have masked even better underlying fatigue performance. Whether similar significant improvements can be achieved in larger panels is for further investigation.

To the best of the authors' knowledge there has been limited research on the topic of CAI fatigue performance improvements using interlaminar toughening technologies. Isa *et al.* [15] carried out a comprehensive study of Z-pinned samples subjected to a range of impact energies between 0J and 25J. It was shown that reinforcing through the thickness using pins reduces the impact damage area for impact energies above 20J only. Above this energy clear improvement in fatigue life was also reported. For lower energies, no significant difference was observed however, with increasing pin density, the CAI strength was reduced in both static and fatigue tests. The fatigue testing from this investigation showed no increase in damage size with fatigue cycle, except at near the failure point. This contrasts with the results of this paper and those from the literature [14,16], where a gradual damage size increase was observed during

the fatigue loading. This may be attributed to the anti-buckling guides being used to prevent any premature out of plane buckling during the compression fatigue tests. With regard to the compression experimental setup used by Isa *et al.* [15], little detail is provided therebfore it is not possible to differentiate the reason for their contrasting results. It is clear that the Z-pins are highly effective at resisting large scale delamination from high impact energy, yet it is the innate reduction in pristine and post-impact compression strength which constrains their wider use in composite structures. In contrast, discrete interleaves have been shown to be beneficial when dealing with low to medium impact energies and thus can provide considerable post-impact compression strength improvements under both static and fatigue loading regimes.

Makeev *et al.* [17] demonstrated that increased shear stress concentration at the ply waviness location around the Z-pin is what determines the effect on the mechanical properties of a composite. This is one reason why Z-pinning inherently reduces the pristine strength of a composite.

The films used in this investigation were manufactured to a nominal thickness of 100μm±25. Embedding this film into the laminate does cause out of plane waviness for the plies in the immediate vicinity of the films, as shown in Figure 11. The severity of this waviness angle depends on the orientation of the fibres relative to the film. Fortunately, the quasi-isotropic layup of the current laminate configuration allows fibres to shift around the embedded films thus reducing fibre waviness angles relative to a unidirectional layup. Furthermore, it has been observed that during the curing process the thermoplastic film becomes soft, thus the autoclave pressure forces the fibres to embed into the film as well as thinning down the edges of the film, which results in no observable resin pockets developing at the film edges. It is believed the

influence of the waviness generated by the embedded films in this current configuration will result in a minor reduction in the pristine composite in-plane strength. Nevertheless, the influence of such waviness angle and film thickness will need to be better understood and is for further investigation.

There are two proposed methods which can reduce the out of plane waviness of the plies around the embedded film as well as minimising any detrimental effects on global stiffness and strength. These are using thinner interleaving films [9] as well as reduced film strip width.

It is expected that the deployment of thinner thermoplastic films will reduce any detrimental effects on pristine in-plane strength due to the combination of reduced ply waviness and smaller resin pocket size that may develop at the film edges. However, the ability to arrest delamination crack will also be affected since the fracture toughness of thinner interleaves is lower [18]. It has been observed that all the delamination cracks have been arrested at the initial edge of the interleaved film (Figure 4 and Figure 5). Thus it is proposed that a narower interleaving strip may be sufficient in arresting delamination cracks thus further minimising the volume of insert materials to be used. The minimum interleaved strip size and its influence on crack arresting capability needs further investigation.

It is appreciated that a reduction in pristine in-plane strength may be a limiting factor preventing the use of such technology in a major composite structure. However, the majority of safety critical composite structures (e.g aerospace) are designed to be tolerant of low velocity impact damage and thus CAI strength is typically a driving factor influencing structural design. Thus making significant improvements to the

impact tolerance of a composite structure using the approach outlined may be highly desirable.

7. Conclusions

The concept for controlling delamination crack damage propagation using discrete interleaved ‘crack arrest’ features has been demonstrated. In this scenario it has been shown that impact damage can be contained or ‘compartmentalised’ and damage propagation effectively managed. Although current practice for composite design in safety critical applications is to employ a ‘no growth’ damage tolerance design philosophy, the hypothesis of this study was to encourage a re-evaluation of this mind set, and explore how damage can be manipulated to manifest itself in predetermined regions, which can then be mitigated by subsequent remedial processes i.e. self-healing.

By employing a parametric study of damage initiation and propagation control, it may be possible to design a composite component with a reduced number of plies which could maintain its structural performance even in the event of significant damage. This could offer a substantial weight saving benefit over current damage tolerant designs for large composite components. Furthermore, combining an ability to manipulate damage growth with an embedded healing capability may facilitate the autonomous repair of damage, effectively prolonging service life.

8. References

[1] Prichard JC, Hogg PJ. “The role of impact damage in post-impact compression testing,” *Composites*, vol. 21, no. 6, pp. 503–511, Nov. 1990.

[2] Liu H, Yan W, Yu X, Mai Y. “Experimental study on effect of loading rate on mode I delamination of z-pin reinforced laminates,” *Composites Science and Technology*, vol. 67, no. 7–8, pp. 1294–1301, Jun. 2007.

[3] Yasaee M, Lander JK, Allegri G, Hallett SR. “Characterisation of bridging mechanisms in a single z-pinned composite laminate,” in *CompTest 2013*, Aalborg, 2013.

[4] Mouritz AP. “Tensile fatigue properties of 3D composites with through-thickness reinforcement,” *Composites Science and Technology*, vol. 68, no. 12, pp. 2503–2510, 2008.

[5] Yasaee M, Bond IP, Trask RS, Greenhalgh ES. “Mode II interfacial toughening through discontinuous interleaves for damage suppression and control,” *Composites Part A: Applied Science and Manufacturing*, vol. 43, no. 1, pp. 121–128, Jan. 2012.

[6] Yasaee M, Bond IP, Trask RS, Greenhalgh ES. “Mode I interfacial toughening through discontinuous interleaves for damage suppression and control,” *Composites Part A: Applied Science and Manufacturing*, vol. 43, no. 1, pp. 198–207, Jan. 2012.

[7] Chang P, Mouritz AP, Cox BN. “Properties and failure mechanisms of z-pinned laminates in monotonic and cyclic tension,” *Composites Part A: Applied Science and Manufacturing*, vol. 37, no. 10, pp. 1501–1513, Oct. 2006.

[8] Sela N, Ishai O. “Interlaminar fracture toughness and toughening of laminated composite materials: a review,” *Composites*, vol. 20, no. 5, pp. 423–435, Sep. 1989.

[9] Yasaee M, Bond IP, Trask RS, Greenhalgh ES. “Damage control using discrete thermoplastic film inserts,” *Composites Part A: Applied Science and Manufacturing*, vol. 43, no. 6, pp. 978–989, 2012.

[10] ASTM-D7136-07. “Standard Test Method for Measuring the Damage Resistance of a Fiber-Reinforced Polymer Matrix Composite to a Drop-Weight Impact Event,” *ASTM International*, 2007.

[11] ASTM D7137-07. “Standard Test Method for Compressive Residual Strength Properties of Damaged Polymer Matrix Composite Plates,” *ASTM International*, 2007.

[12] McCombe GP, Rouse J, Trask RS, Withers PJ, Bond IP. “X-ray damage characterisation in self-healing fibre reinforced polymers,” *Composites Part A: Applied Science and Manufacturing*, vol. 43, no. 4, pp. 613–620, Apr. 2012.

[13] Nilsson KF, Asp LE, Alpman JE, Nystedt L. “Delamination buckling and growth for delaminations at different depths in a slender composite panel,” *International Journal of Solids and Structures*, vol. 38, no. 17, pp. 3039–3071, Apr. 2001.

[14] Butler R, Almond D, Hunt G, Hu B, Gathercole N. “Compressive fatigue limit of impact damaged composite laminates,” *Composites Part A: Applied Science and Manufacturing*, vol. 38, no. 4, pp. 1211–1215, Apr. 2007.

[15] Isa MD, Feih S, Mouritz a. P. “Compression fatigue properties of z-pinned quasi-isotropic carbon/epoxy laminate with barely visible impact damage,” *Composite Structures*, vol. 93, no. 9, pp. 2269–2276, Aug. 2011.

[16] Melin LG, Schön J. “Buckling behaviour and delamination growth in impacted composite specimens under fatigue load: an experimental study,” *Composites science and technology*, vol. 61, no. 13, pp. 1841–1852, Oct. 2001.

[17] Makeev A, Seon G, Lee E. “Failure predictions for carbon/epoxy tape laminates with wavy plies,” *Journal of composite materials*, vol. 44, no. 1, pp. 95–112, Sep. 2010.

[18] Sela N, Ishai O, Bankssills L. “The effect of adhesive thickness on interlaminar fracture toughness of interleaved cfrp specimens,” *Composites*, vol. 20, no. 3, pp. 257–264, May 1989.

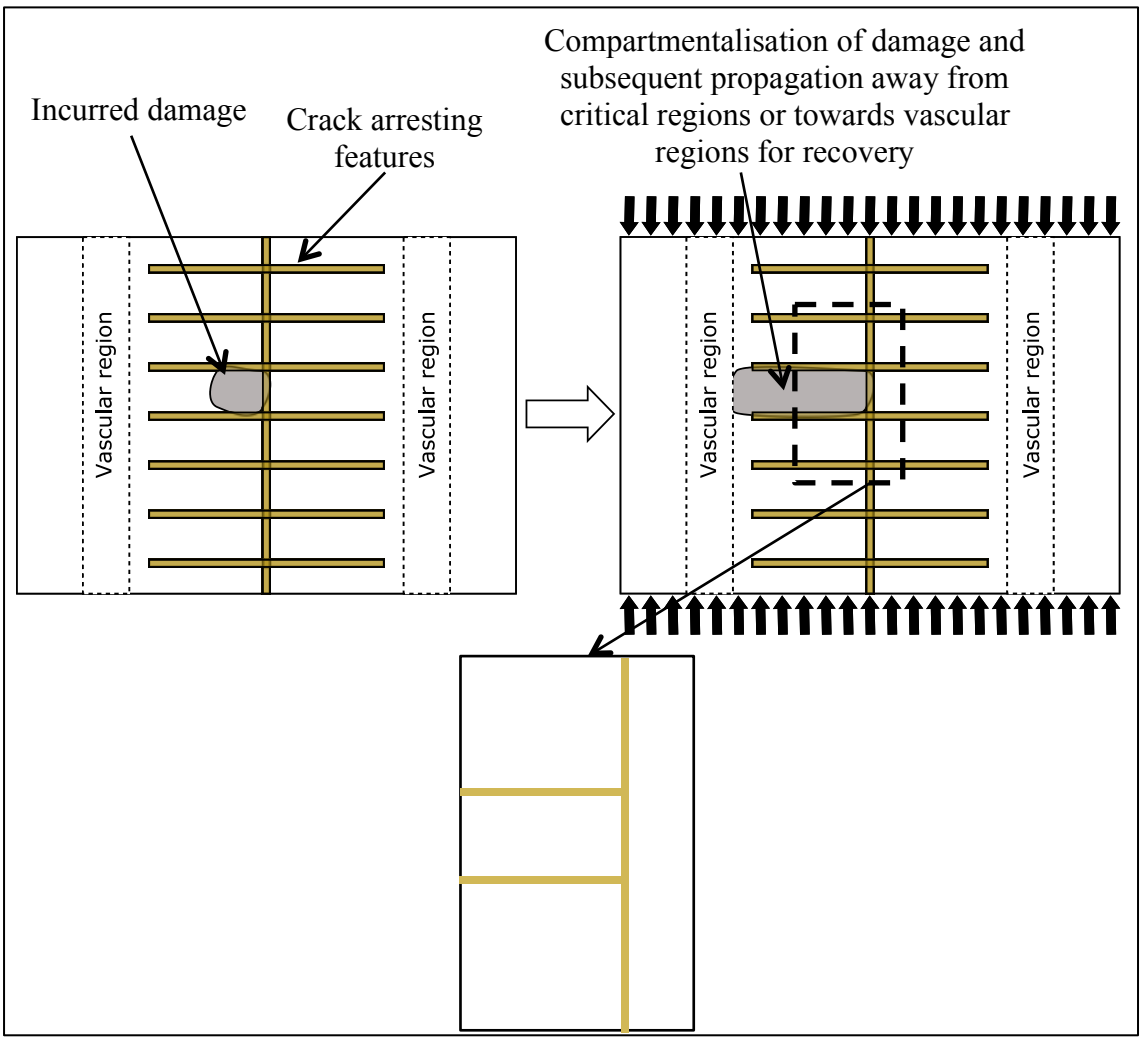

Figure 1 Damage propagation control concept

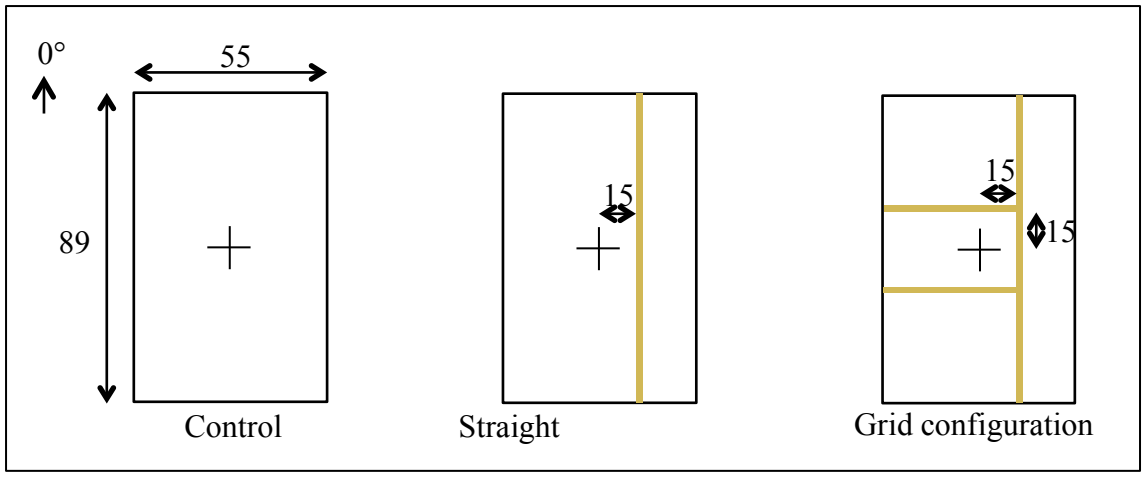

Figure 2 CAI panel configurations embedded with 2.5mm interleaved strips indicating their position relative to impact point (dimensions in mm)

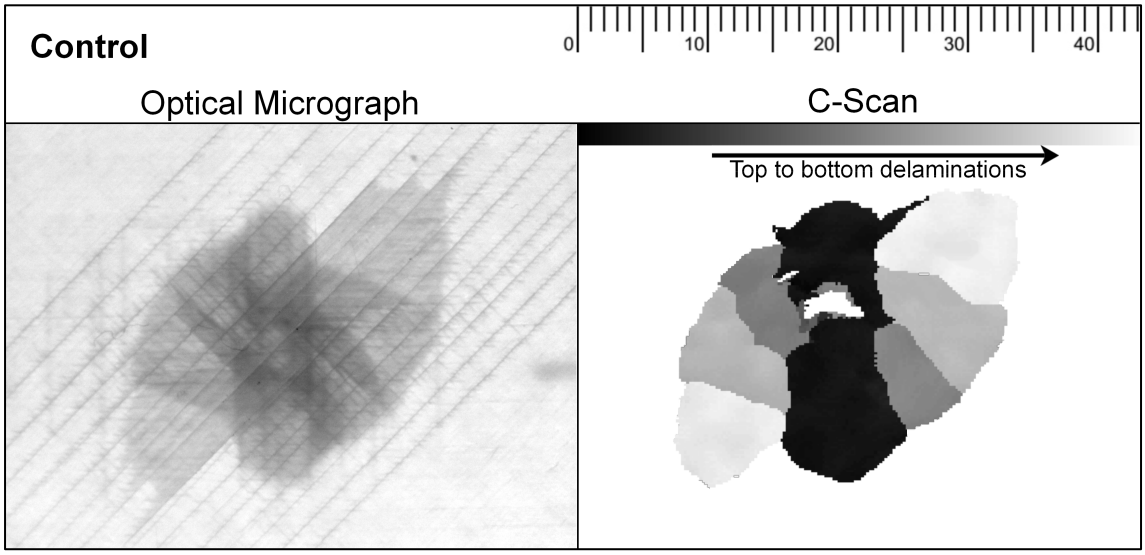

Figure 3 Optical and C-scan micrographs of the control panel subjected to an 15J impact

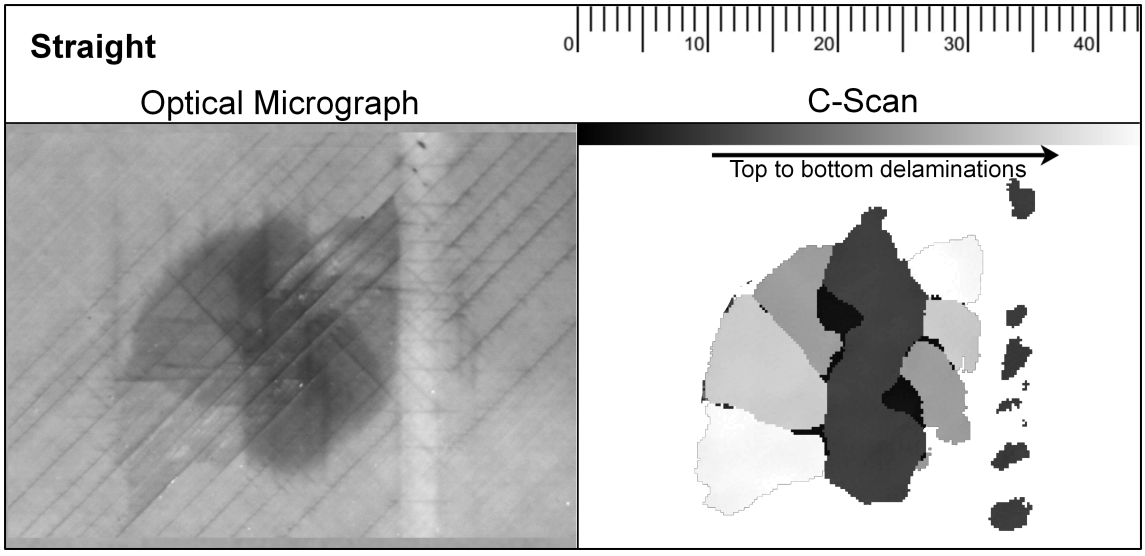

Figure 4 Optical and C-scan micrographs of the straight configuration panel subjected to a 15J impact

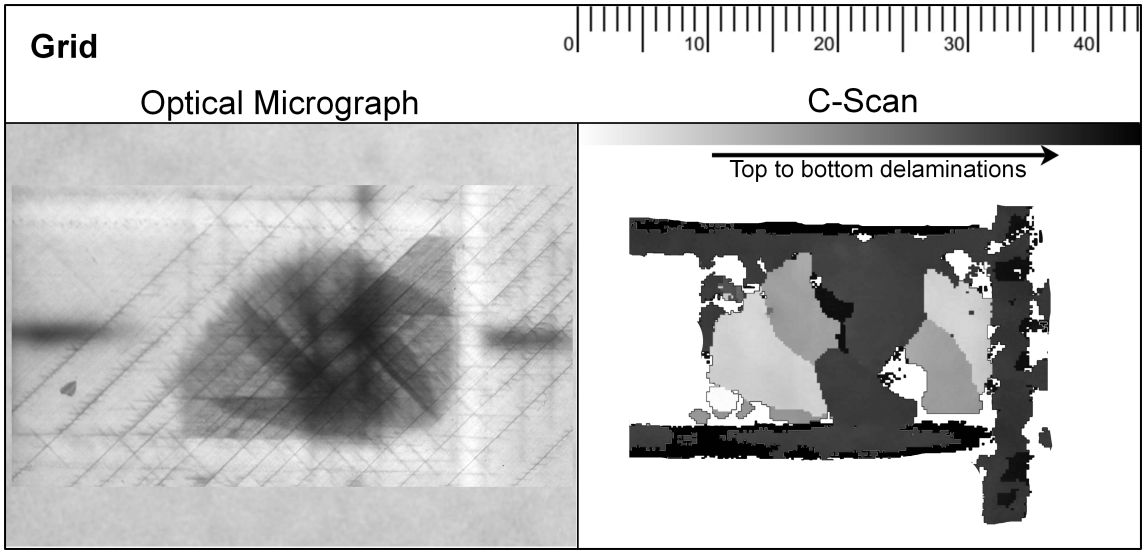

Figure 5 Optical and C-scan micrographs of the grid configuration panel subjected to a 15J impact

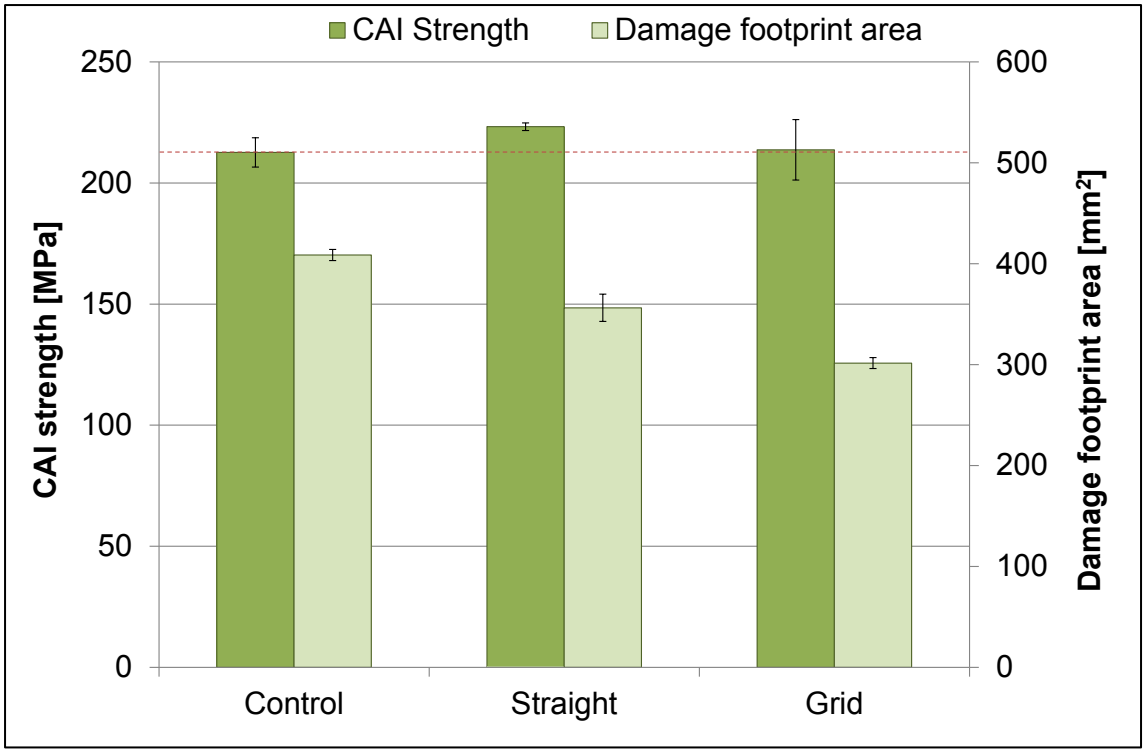

Figure 6 Averaged Compression After Impact (CAI) strength and damage footprint area of the three configurations (error bars equal one standard deviation, 3 samples per data point)

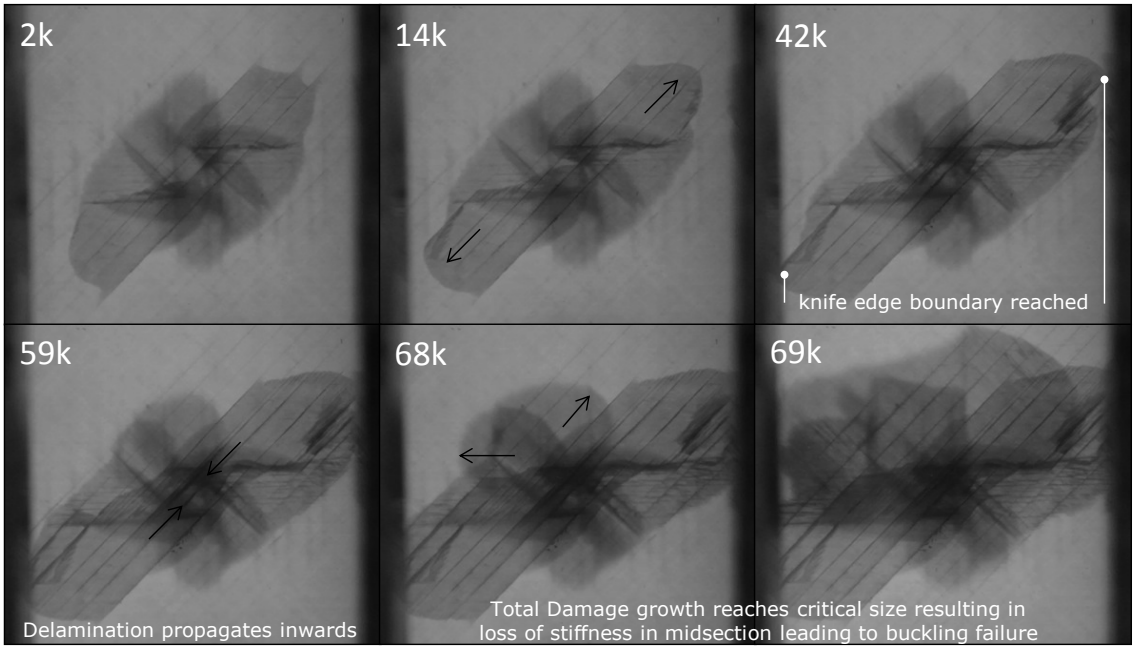

Figure 7 Representative sample of control configuration showing delamination growth during fatigue cycle

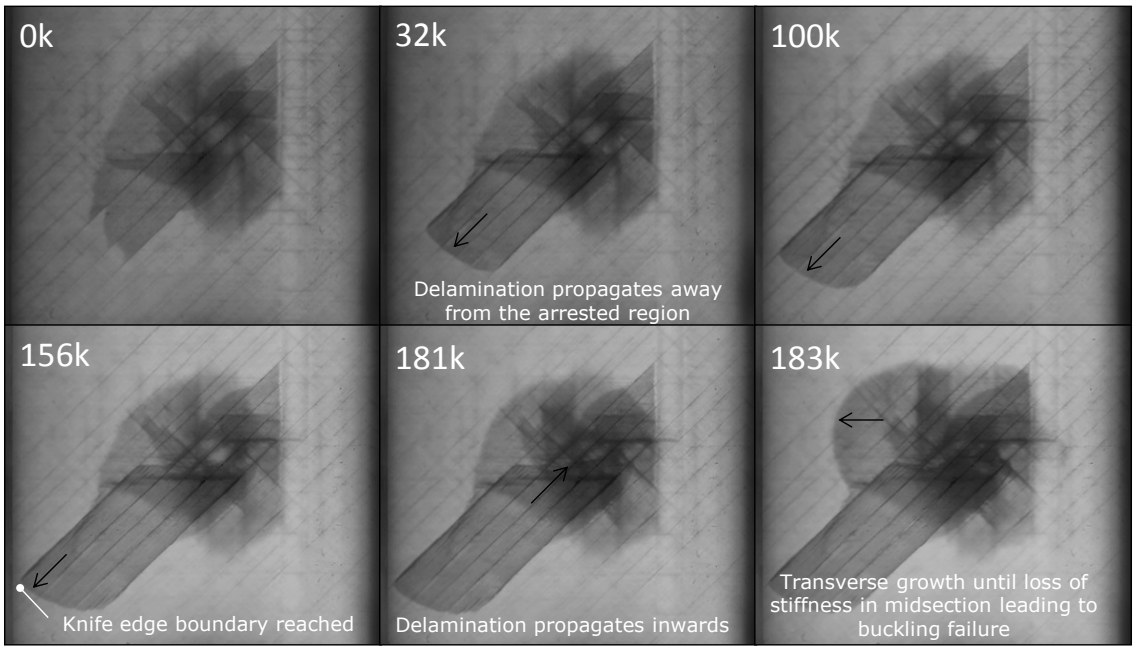

Figure 8 Representative sample of straight configuration showing delamination growth during fatigue cycle

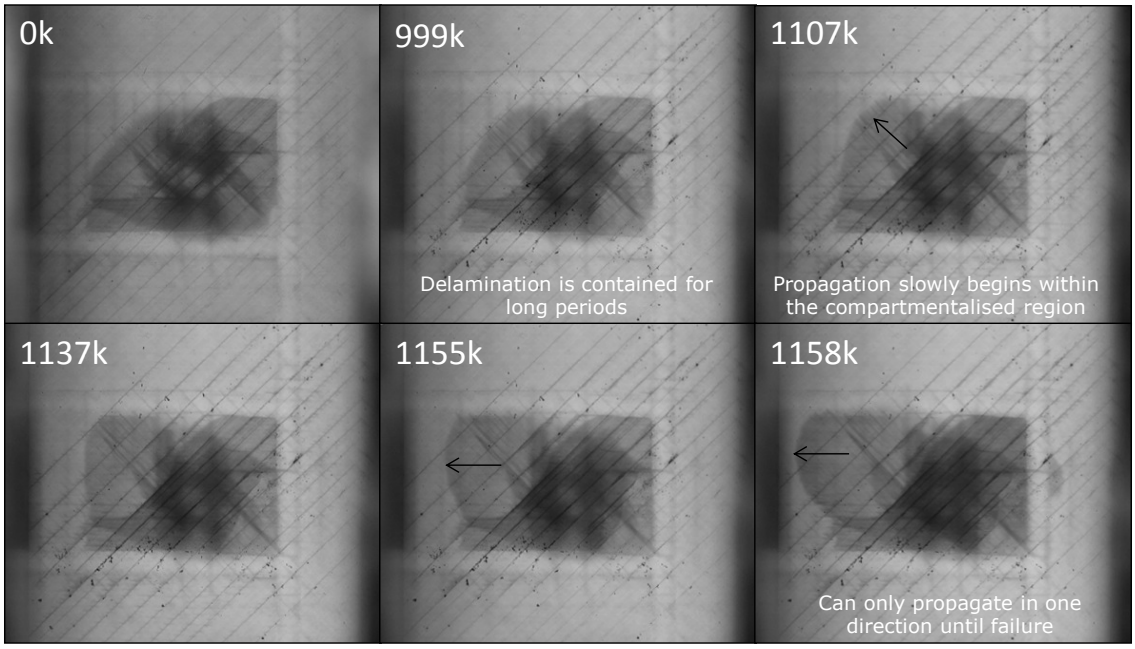

Figure 9 Representative sample of grid configuration showing delamination growth during fatigue cycle

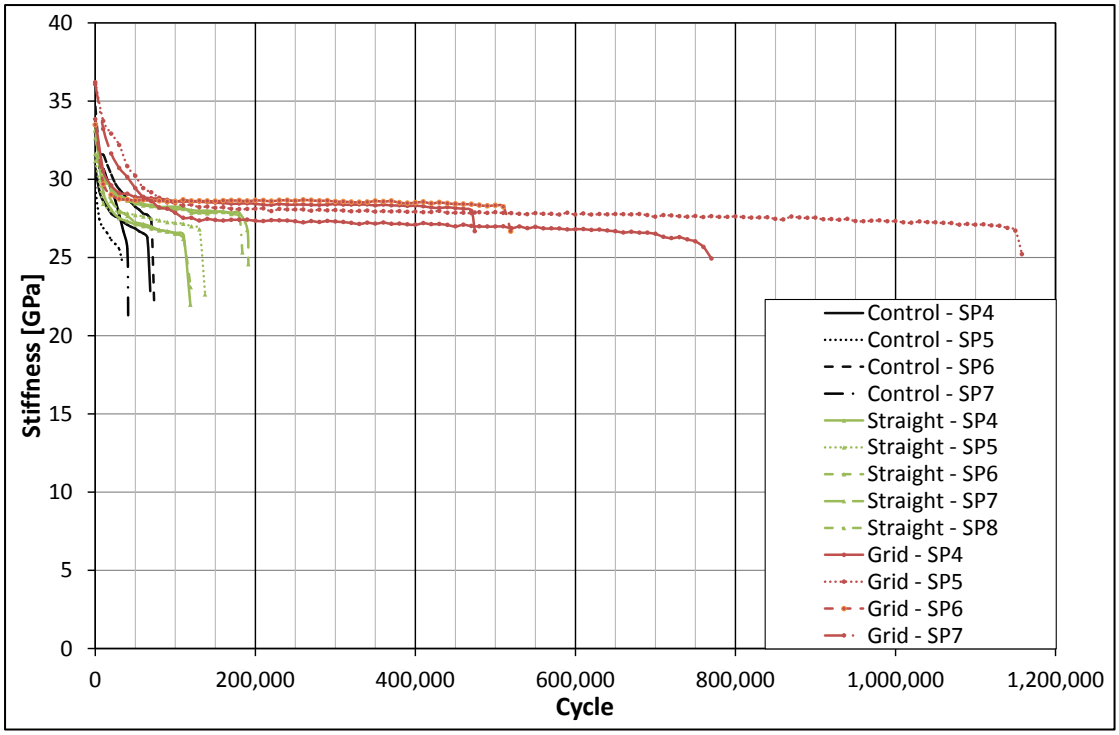

Figure 10 Stiffness degradation as a function of fatigue cycles (5Hz C-C fatigue cycle at ~81% static limit load with R=11)

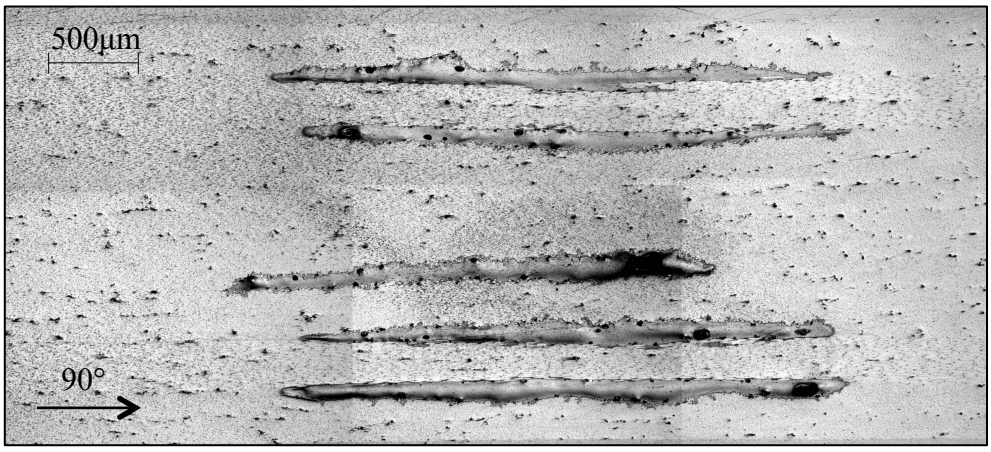

Figure 11 Cross section optical micrograph showing the through thickness distribution of the vertically aligned interleaves

Table 1 Layup configuration indicating the interleaved position and orientation, horizontal (H) and vertical (V)

Ply angle	Interface	Grid	Straight
45°		Impact Face	
	1	V	V
90°			
	2	H+V	V
-45°			
	3	H	
0°			

0°			
	4	H+V	V
-45°			
	5	V	V
90°			
	6	H+V	V
45°		Back Face	

Table 2 C-C fatigue cycles to failure results

	Sample					Average
	4	**5**	**6**	**7**	**8**	
Control	68,700	33,700	73,600	41,100	-----	**54,275**
Straight	118,800	137,300	119,200	191,300	183,800	**150,080**
Grid	474,400	1,158,120	519,400	770,100	-----	**730,505**